Astron. Nachr./AN **32X** (200X) X, XXX–XXX

The Chandra Multi-wavelength Project (ChaMP): Results and Prospects

PAUL J. GREEN[1,*], ROB CAMERON[1,*], HIMEL GHOSH[1], JOHN GRIMES[1], DONG-WOO KIM[1], DAVID MORRIS[1], AMY MOSSMAN[1], JOHN SILVERMAN[1,*], BELINDA WILKES[1], JACK BALDWIN[3], BUELL JANNUZI[2], RICK HARNDEN[1], VINAY KASHYAP[1], AARON LACLUYZÉ[3,*], PETER MAKSYM[1], ERIC SCHLEGEL[1], HARVEY TANANBAUM[1], ALEXEY VIKHLININ[1], CHRIS SMITH[2], MALCOLM SMITH[2] and THE CHAMP COLLABORATION

[1] Smithsonian Astrophysical Observatory, 60 Garden St., Cambridge, MA 02138
[2] National Optical Astronomy Observatory, P.O. Box 26732, Tucson, AZ, 85726-6732
[3] Department of Physics and Astronomy, Michigan State University, East Lansing, MI 48824-1116

Received *date will be inserted by the editor*; accepted *date will be inserted by the editor*

Abstract. The cosmic diffuse X-ray background radiation has been almost completely resolved into point sources by Chandra and XMM. However, the nature and evolution of those sources are just beginning to be investigated. The answers are key to our understanding of the inter-relationship over cosmic time of (a) the formation and growth of black holes, (b) star formation, and (c) hierarchical structure formation. This requires multiwavelength followup of Chandra sources over a large area. The Chandra Multiwavelength Project (ChaMP) is a serendipitous survey of the X-ray sky, covering about 14 $\deg^2$ of sky in the X-ray flux range of -13 to -16 (log 0.5-2 keV flux, cgs) and will include about 8000 sources, 70% of which are expected to be active galactic nuclei (AGN). Using Chandra archival data, we span flux limits between those reached by previous satellites and those of the deepest small-area Chandra and XMM surveys, allowing study of larger samples of rare objects like luminous absorbed AGN, groups and clusters of galaxies, and their spatial correlations. Optical imaging and spectroscopy of the ChaMP fields are underway at a variety of telescopes using Sloan g', r', and i' filters to a flux limit matched to the X-ray such that about 75% of the X-ray sources will be optically identified. We also plan for radio and near-IR observations of subsets of the ChaMP sample to expand our multi-wavelength coverage and increase the fraction of sources identified.

Key words: X-rays — surveys — quasars: general

1. Introduction

As amply argued in this volume, X-ray surveys provide fundamental advances in our knowledge of the X-ray universe and indeed the universe as a whole. Chandra and XMM have resolved 80-90% of the cosmic X-ray background (CXRB) into discrete sources (e.g., Cowie et al. 2002; Rosati et al. 2002), most of which are likely to be active galactic nuclei (AGN). However, the high energy spectrum of the CXRB is much harder ($\Gamma \sim 1.4$; Chen et al. 1997) than that of known AGN ($\Gamma \sim 1.9$). Population synthesis models that satisfy both the CXRB spectrum and the observed X-ray number counts vs. flux relation (log*N*-log*S*; e.g., Gilli et al. 2002) favor absorbed AGN (where circumnuclear gas absorbs low energy X-rays) as a dominant component of the CXRB, whereby *most* of the accretion luminosity in the universe is from obscured sources. Most past surveys for AGN, however are biased against finding these sources. Traditional soft X-ray and optical surveys suffer strong selection effects due to intrinsic obscuration and the intervening Lyα forest. The bright optical quasar population falls dramatically on either side of $z \sim 2.5$. Preliminary evidence from deep soft X-ray surveys (Miyaji et al. 2000) indicates that the co-moving space density of X-ray-selected quasars may not drop off towards higher z as in optically-selected samples. But greater (especially hard) X-ray sensitivity is needed. For *Chandra* and *XMM,* sensitivity to emission up to 10 keV (observed frame) can reveal hidden populations of active galactic nu-

Correspondence to: pgreen@cfa.harvard.edu

* Visiting Astronomer, Kitt Peak National Observatory and/or Cerro Tololo Inter-American Observatory, National Optical Astronomy Observatories, operated by the Association of Universities for Research in Astronomy, Inc. (AURA) under cooperative agreement with the National Science Foundation.

clei (AGN) including heavily obscured quasars. Followup at other wavelengths is critical to characterizing the source population. Optical and X-ray surveys complement each other, providing a fair census of mass accretion onto black holes at high redshift. Now, with its low background and tight PSF ($\leq 1''$ FWHM on axis) *Chandra* is probing the high energy universe with unparalleled sensitivity and resolution.

The greatest contribution to the CXRB comes from relatively bright sources ($f_{2-10\mathrm{keV}} \sim 10^{-14}$cgs; Cowie et al. 2002). With just ~ 32 such objects per deg^2, a large number of Chandra fields are required to probe the population. High L_X ($> 2 \times 10^{44}$ cgs), highly absorbed objects are required to reproduced the (2-10keV) source counts at these fluxes. Though they are ardently sought as the so-called Type 2 QSOs - the elusive high luminosity version of Seyfert 2 galaxies - few of these have been convincingly detected to date Akiyama, M., Ueda, Y., & Ohta, K. 2002; Stern, D., et al. 2002). Most of the hard sources from *Chandra* and XMM Newton surveys are objects at $z < 2$ (Barger et al. 2002), which requires a very different evolution rate for absorbed and unabsorbed objects. This population needs a great deal more study, but to find a statistically significant number of such objects requires a wide, medium-depth X-ray survey.

2. Field Selection and Survey Predictions

The ChaMP field selection includes Chandra Cycle 1 and 2 archival images from high latitudes ($|b| > 20°$), and requires that at least 4 full ACIS CCD chips be turned on. We exclude fields with bright optical or X-ray sources or objects covering $> 10\%$ of the *Chandra* image, or fields intended for serendipitous surveys. The result is about 144 ACIS fields. In Figure 1, we show our estimate of the number of sources expected in the full ChaMP survey. We first simulate the number of sources detected in each *Chandra* image by randomly populating the CCDs with sources derived from the log*N*-log*S*, assuming an average spectral slope $\Gamma = 1.4$. We take into account the known CCD QE and background count rates, the mirror PSF and vignetting through analytic fits. We expect a total of about 8000 sources from all fields.

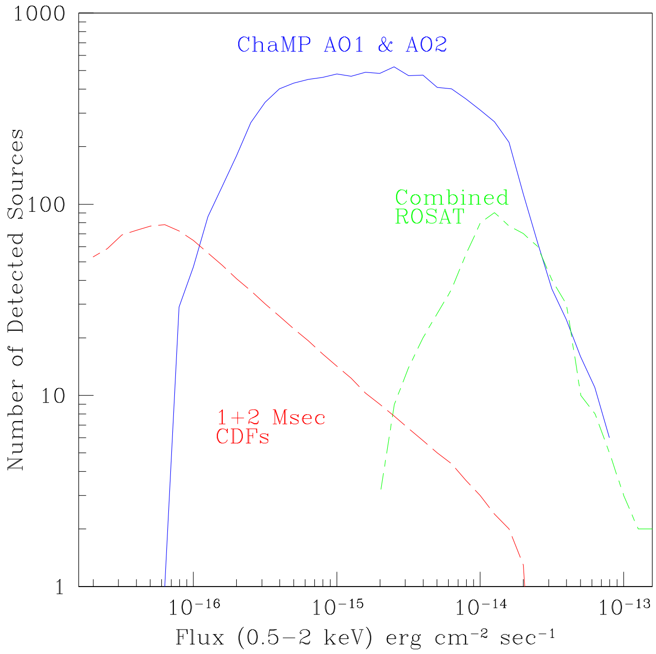

Fig. 1. ChaMP Predicted Number Counts Predicted number (2σ) of sources detected for the 6 fields in this paper, and for 135 ChaMP Cycle 1+2 fields, based on a deep log*N*-log*S*. Also included are the same simulation for the combined CDFs (2Msec North and 1Msec South), and 690 sources from 7 combined ROSAT surveys analyzed by Miyaji et al. (2000).

3. X-ray Results

The foundation of the ChaMP rests on our own *Chandra* image analysis pipeline XPIPE (Kim et al. 2003), built mainly with CIAO tools (http://asc.harvard.edu/ciao), and designed to uniformly and carefully screen and analyze the X-ray data. At the source positions determined by CIAO `wavdetect` centroid, we perform our own aperture photometry. We use a circular source aperture whose radius encompasses 95% of deposited energy, determined at 1.5keV, but restrict this radius to the range $3'' < r_{ap} < 40''$. We compute fluxes for each source taking vignetting and its energy dependence into account, assuming a power-law of photon index $\Gamma = 1.4$ absorbed only by a neutral Galactic column density.

The flux regime where the ChaMP has greatest sky area coincides with the break near 10^{-14}erg cm^{-2} s^{-1} between power-law slopes in the hard (2-10keV) log*N*-log*S*(Rosati et al. 2002). Figure 2 illustrates that at these fluxes, the gap in coverage between deep ASCA and *Chandra* surveys is now filled by the medium depth and wide area of *Chandra* fields included in the ChaMP.

To gain a fair measure of the X-ray spectral properties of every source, we calculate a hardness ratio $HR = \frac{H-S}{H+S}$ referenced to a source on-axis on a front-illuminated (FI) chip. Many (especially weak) sources have raw H or S counts that are formally $< 2\sigma$, or even negative. Naïve inclusion of these yields nonsensical HR values outside the physical range from -1 to 1. Therefore, we first replace such counts by a 2σ upper limit. Figure 3 shows HR values both raw, and corrected as just described. Previous studies have often assumed that when total source counts exceed 30 or 50, that the HR values are reliable. In fact, the fraction of (mostly upper) limits to hardness decreases below 10% only above about 120 broad (0.3-8keV) band counts. Correctly incorporating the upper limits via survival analysis (LaValley, Isobe & Feigelson 1992), we find no significant evidence for hardening of the spectra toward lower fluxes.

4. Optical Imaging

As detailed in Green et al. (2003), optical imaging is crucial to provide optical fluxes, preliminary source classification, and accurate centroiding for spectroscopic followup. Multiband colors provide source classifications and photometric redshifts for the majority of fainter ChaMP sources ($r' > 22$) for which high quality spectra are more difficult to obtain. We

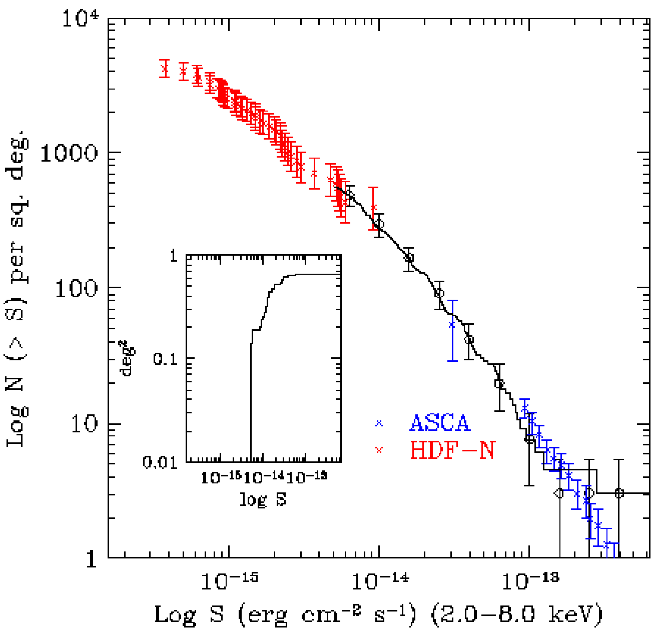

Fig. 2. ChaMP cumulative source counts as a function of (2-8keV) flux for high confidence (counts > 20) sources in the inner 400″ of 62 ChaMP fields analyzed by Kim et al. (2003). New ChaMP points (open circles joined by the histogram) are consistent with previous findings, yet bridge the gap in flux nearest the region that dominates the CXRB (Cowie et al. (2002). Data points at low flux are from the Chandra Deep Field North (Brandt et al. 2002), and at high fluxes from ASCA (Ueda et al. 1998). The inset shows the effective sky area as a function of flux limit for this ChaMP subsample.

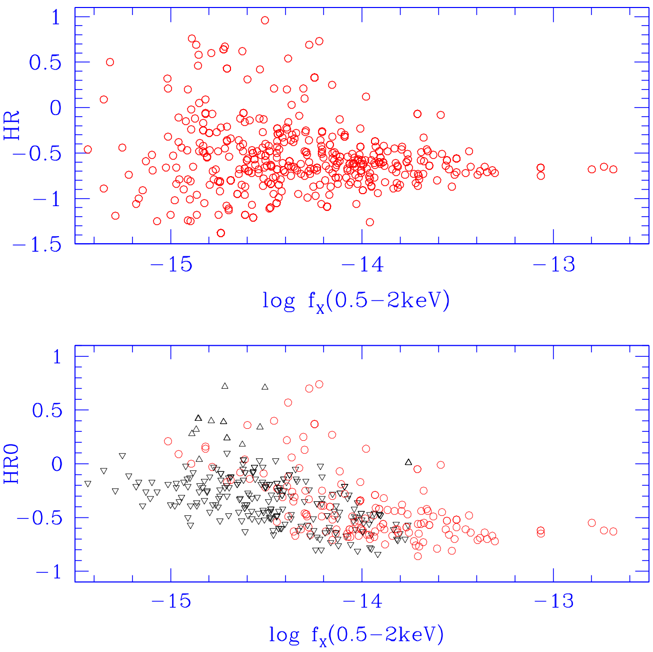

Fig. 3. TOP: Raw hardness ratios HR plotted as a function of X-ray flux. Many non-physical values ($HR < -1$) are seen, particularly at low fluxes. BOTTOM: Corrected hardness ratios $HR0$ plotted as a function of X-ray flux. HR values are corrected to represent a source on-axis on a front-illuminated (FI) chip. Triangles represent upper or lower limits to $HR0$, based on 2σ upper limits to H or S counts, respectively.

convert 10 on-axis counts for each *Chandra* field to an X-ray flux limit, and then scale the corresponding optical magnitude limit based on $\log(f_X/f_V) = 0.9$, which includes > 90% of ROSAT AGN even at the X-ray flux limit[1] The resulting limits range from V mags (note that $V \sim (g' + r')/2$) of 21 to 26 with a median of 23.5mag for all ChaMP fields (and 24.7mag for 4m fields). However, to achieve reasonable limits on the amount of required optical imaging time, we limit our maximum optical depth to $V \sim 25$. We primarily use the NOAO 4-meter telescopes with MOSAIC CCD cameras for the ChaMP, since it provides adequate depths and spatial resolution ($\sim 0.26''$/pixel), but also - with $36'$ on a side - covers the full *Chandra* field of view. Three Sloan Digital Sky Survey (SDSS) g', r', and i' filters are used, since their steep transmission cutoffs improve object classification and photometric redshift determination. The IRAF[2] package `mscred` is used to properly handle the multi-extension FITS images and to simplify the data reduction. Optical sources are referenced to the Guide Star Catalog II.[3] We use SExtractor (Bertin & Arnouts 1996) to detect sources, and measure positions and magnitudes. We merge instrumental magnitudes from each filter into a multicolor file by (1″) positional cross-correlation before photometric calibration.

[1] Based on 1448 ROSAT-detected quasars from Yuan et al. (1998).

[2] IRAF is distributed by the National Optical Astronomy Observatory, which is operated by the Association of Universities for Research in Astronomy, Inc., under cooperative agreement with the National Science Foundation.

[3] The Guide Star Catalogue-II is a joint project of the Space Telescope Science Institute and the Osservatorio Astronomico di Torino.

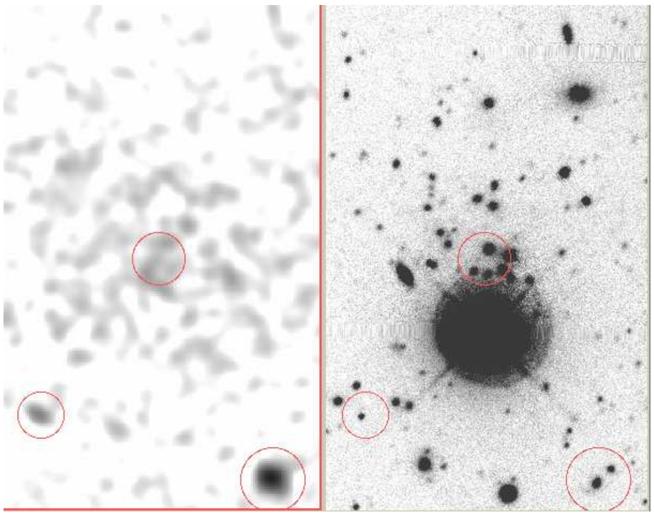

Fig. 4. LEFT: We noted extended X-ray emission in a 40ksec ChaMP field. The field is approximately 2′ NS, and 1.3arcmin EW, with N up and E to the left. Circles show the positions of detected X-ray sources, with circle size corresponding to the *Chandra* 95% encircled energy at this off-axis angle. RIGHT: As expected for any significantly extended high galactic latitude X-ray source, our CTIO4m/MOSAIC imaging indeed shows a cluster of galaxies just N of a $V = 12$ star. The $r' = 21$ optical object close to the X-ray centroid is a $z = 0.467$ NELG from our (2001 Oct 16) CTIO4m/Hydra spectroscopy.

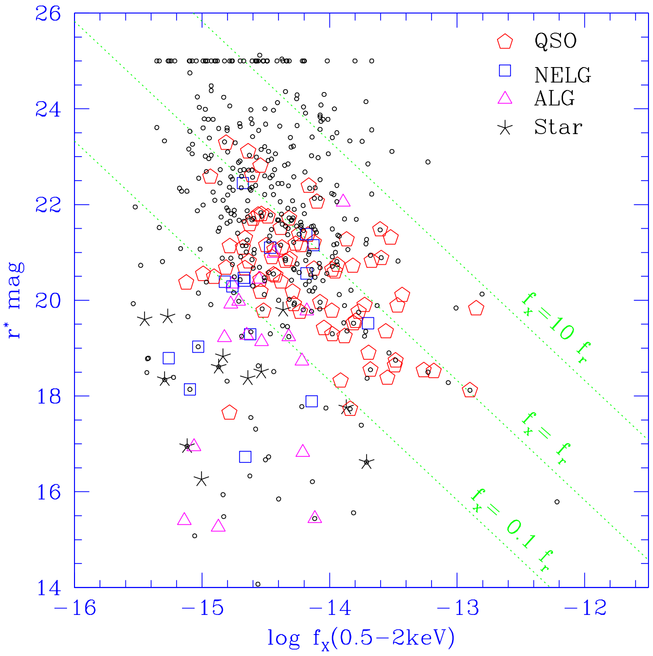

Fig. 5. SDSS r' band magnitudes vs. log f_x in the 0.5–2 keV band for all matched sources in the 6 fields studied here. Overplotted are 3 lines of constant $\frac{f_x}{f_r}$ at 0.1, 1, and 10. Large symbols are shown for spectroscopically classified sources. QSOs are limited to $\frac{f_x}{f_r} > 0.1$. Galaxies tend to appear towards fainter X-ray fluxes but span a wide range of optical brightness. Stars are essentially limited to $r' < 20$, which corresponds to a typical M dwarf between at $400 - 1000$pc. Sources without optical counterparts are plotted at $r' = 25$, slightly fainter than our mag limit in these fields.

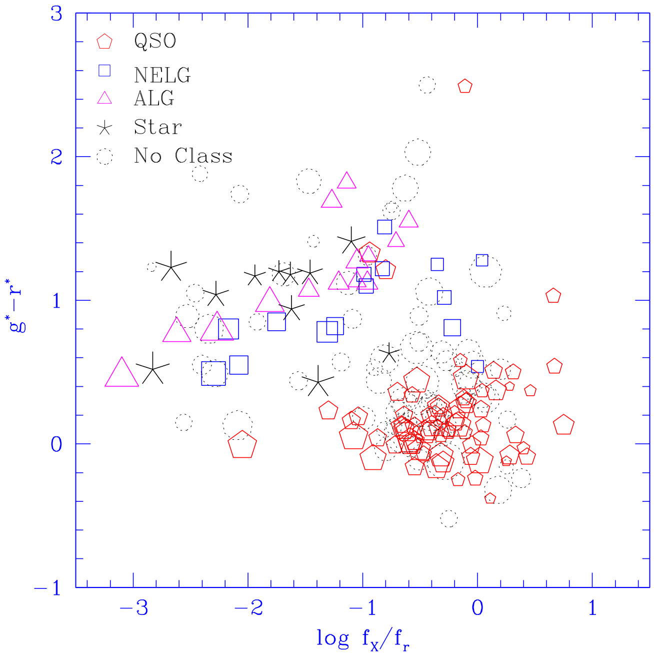

Fig. 6. SDSS $(g' - r')$ colors derived from our MOSAIC imaging vs. log $(\frac{f_x}{f_r})$ in the 0.5–2 keV band. Here, symbol size is proportional to optical brightness. The strongest clustering is of QSOs at high log $(\frac{f_x}{f_r})$ and blue $(g' - r')$ colors. Objects in this part of the plot can be classified as QSOs with high confidence even without spectroscopy.

5. Optical Counterparts

After our automated O/X matching between detected sources from XPIPE and SExtractor has been performed, we examine the images by eye. The small PSF and accurate centroiding of *Chandra* become crucial at these faint magnitudes, as does careful source inspection. As showin in Figure 4, we occasionally find a single X-ray source that is extended (larger than the expected PSF) and has several possible optical counterparts. These are galaxy clusters; we find about one in every 3 deep ($>$ 30ksec) ChaMP fields. We expect the ChaMP to yield perhaps 30 such high L_X clusters at redshifts out to unity.

For each source, we calculate a simple X-ray to optical flux ratio using our SDSS r' magnitudes: $\log\frac{f_X}{f_r} = \log f_X + 5.67 + 0.4r'$. Figure 5 shows a plot of the r' magnitude against log f_x in the 0.5–2 keV band. Overplotted are 3 lines of constant log $(\frac{f_x}{f_r})$ at -1, 0, and 1.

Silverman et al. (this volume) describes in detail how our optical spectroscopy efforts are segregated broadly into 3 magnitude regimes. The majority of sources with optical counterparts are fainter than our spectroscopic limit. A true multi-parameter photometric characterization has great promise both for classification and photometric redshift estimates of these faint sources. By including fluxes, colors, and morphological information both from X-ray and optical imaging, the ChaMP will greatly extend our knowledge of faint X-ray sources from redshifts 0 to 6, applicable both to the history of black hole accretion and the evolution of star formation in the universe. Information about the ChaMP, and a growing database of images and results can be accessed at http://hea-www.harvard.edu/CHAMP/

Acknowledgements. Hearty thanks to the whole *Chandra* team for a wonderful telescope and offering top-notch archival research support. Thanks to all those whose names cannot appear here who work so hard on the many aspects of the ChaMP. We gratefully acknowledge the financial support of NASA grant AR1-2003X (Chandra).

References

Akiyama, M., Ueda, Y., & Ohta, K. 2002, ApJ, in press
Barger, A. J. et al. 2001, AJ, 124, 1839
Bertin, E. & Arnouts, S. 1996 A&AS 117, 393
Brandt, W. N. et al. 2001, AJ, 122, 2810
Chen, L.-W., Fabian, A.C. & Gendreau, K.C. 1997, MNRAS, 285, 449
Cowie, L. et al. 2002, ApJL, 566, L8
Green, P. J. et al. 2003, ApJ, submitted
Kim, D.-W. et al. 2003, in preparation
LaValley, M., Isobe, T., & Feigelson, E.D. 1992, in Astronomical Data Analysis Software and Systems, ed. D. Worrall et al. (San Francisco: ASP)
Miyaji et al. 2000, A&A, 353, 25
Rosati, P., et al. 2002, ApJ, 566, 667
Stern, D., et al. 2002, ApJ, 568, 71
Ueda, Y. et al. 1998, Nature, 391, 866
Yuan, W., Brinkmann, W., Siebert, J., & Voges, W. 1998, A&A, 330, 108